Synthesis and Crystal Structure of Ag_4I_4 Nanoclusters in the Sodalite Cavities of Fully K^+-Exchanged Zeolite A

Nam Ho Heo* and Han Soo Kim

Laboratory of Structural Chemistry, Department of Industrial Chemistry, Kyungpook National University, Taegu 702-701, Korea

Woo Taik Lim

Department of Applied Chemistry, Andong National University, Andong 760-749, Korea

Karl Seff*

Department of Chemistry, University of Hawaii at Manoa, Honolulu, Hawaii 96822-2275

Received: October 3, 2003

Ag_4I_4 nanoclusters have been synthesized in half of the sodalite cavities of fully K^+-exchanged zeolite A. An additional KI molecule is retained in each large cavity as part of a near square planar K_4I^{3+} cation. A single crystal of Ag_{12}-A, prepared by the dynamic ion-exchange of Na_{12}-A (LTA) with aqueous 0.05 M $AgNO_3$ and washed with CH_3OH, was placed in a stream of flowing 0.05 M KI in CH_3OH at 294 K for 2 days. The crystal structure of the product, $K_9Si_{12}Al_{12}O_{48}\cdot(Ag_4I_4)_{0.5}\cdot K_4I^{3+}$, $a = 12.290(1)$ Å, was determined by single-crystal X-ray diffraction in the cubic space group $Pm\bar{3}m$. It was refined with all measured reflections to the final error index $R_1 = 0.077$ (based on the 264 reflections for which $F_o > 4\sigma(F_o)$). The thirteen K^+ ions per unit cell are found at three crystallographically distinct positions: eight K^+ ions in the large cavity fill the 6-ring site, three K^+ ions fill the 8-rings, and two K^+ ions are opposite 4-rings in the large cavity. One iodide ion per unit cell lies opposite a 4-ring in the large cavity, held there by two 8-ring and the two 6-ring K^+ ions (K_4I^{3+}). Two Ag^+ and two I^- ions per unit cell are found on 3-fold axes in the sodalite cavity, indicating the formation of Ag_4I_4 clusters (interpenetrating tetrahedra; symmetry T_d; diameter *ca.* 8.0 Å) in half of the sodalite units. Each cluster ($Ag-I = 2.97(2)$ Å) is held in place by the coordination of its four Ag^+ ions to the zeolite framework (each Ag^+ cation is 2.48(1) Å from three 6-ring oxygens) and by the coordination of its four I^- ions to large-cavity K^+ ions through 6-rings ($I-K = 2.72(6)$ Å).

Introduction

Zeolites, because of their regular pore and channel systems, are potentially useful for the stabilization of unusual chemical species and finely dispersed bulk materials.[1,2] They can be good supports or carriers for particles up to ca. one nanometer in diameter and can stabilize these nanoclusters under ambient conditions. (Mesoporous materials may be expected to stabilize larger nanoclusters.) Zeolites can require nanoclusters to be both uniform in size and regular in orientation.[3−9]

Because of their photosensitive properties (e.g., AgBr-based photography), bulk silver halides are unique semiconductors.[10−12] They are very sensitive to light and may find application as photocatalysts for solar energy conversion and as media for optical information or image storage.[13] The incorporation of silver halides into zeolites should yield regular arrays of nanosized clusters with quantum-size (quantum-confinement) effects.[3,14] Additionally, silver halides in zeolites have photostimulated luminescence (PSL) properties,[15] and these zeolites may be used as image plates for computerized X-ray radiography or for erasable optical memory.[15] Takushi Hirono et al.[16] proposed that a silver halide dispersed in a large-pore zeolite could function as an optical recording medium. They claimed that the material would darken when exposed to light and expected that it would fade back to its original color on heating.

G. A. Ozin et al.[10,17] extensively studied the synthesis, structure, and spectroscopic properties of silver halide clusters in various halosodalites. In all cases, these were Ag_4X^{3+} clusters.

Takushi Hirono et al.[18] synthesized a mordenite-AgI inclusion complex by sintering a mixture of mordenite and AgI in air at 773 K for about 50 h. They described its unusual interaction with Ar laser light. They observed an absorption process which was followed, after a certain period of irradiation, by transitory luminescence. They proposed that the photosensitization had an irradiation power-density threshold instead of the energy-density threshold usually observed in many photosensitive materials. These characteristics were not observed in bulk AgI.

Wei Chen et al.[13] studied the photostimulated luminescence (PSL) of silver iodide clusters in zeolite Y. They demonstrated that silver iodide clusters encapsulated in zeolites may work as a medium for erasable optical memory. To prepare these clusters, they first exchanged Ag^+ ions into the zeolite. The zeolite Y powder was then slurried with aqueous sodium iodide by stirring at 100 °C for 20 h.

On the basis of optical absorption spectra, T. Kodaira et al.[12] discussed the electronic states and structures of the AgI clusters prepared by the direct absorption of bulk AgI into zeolite Na-A. X-ray powder diffraction patterns were seen to depend on the loading density of AgI in the range from 0.2 to 4.0 molecules per 12.3-Å unit cell. They suggested that $(AgI)_n$ clusters, where

* Corresponding authors. E-mail: nhheo@knu.ac.kr; seff@hawaii.edu

10.1021/jp031137p CCC: $27.50
Published on Web 01/31/2004

n ranges from two to four, form in α-cages with increasing loading density, and that the clusters occupy positions of tetrahedral symmetry in the α-cage.

Nanoscale silver iodide guests were introduced into zeolites Na−ZSM5 and Na−Y by Qing-Zhou Zhai et al.[19] who studied their products using powder X-ray diffraction (XRD), differential thermal analysis (DTA), X-ray photoelectron spectroscopy (XPS), and inert-gas adsorption techniques (to define the placement of the silver iodide). They prepared their host−guest nanocomposite materials Na−Y·AgI and Na−ZSM5·AgI by a thermal diffusion method and observed the quantum confinement effect of the zeolite channels and cavities.

Hirono et al.,[18] Chen et al.,[13] Kodaira et al.,[12] and Zhai et al.[19] have shown that silver iodide can be introduced into the body of a zeolite. In each study, the materials synthesized were characterized and additional physical measurements were made as indicated above. However, in no case was the placement of the nanoclusters determined, nor were the structures of the nanoclusters determined, nor was it established for any sample that the nanoclusters were uniform in size. In addition, the results reported herein for zeolite A suggest that their silver iodide clusters were in the sodalite cavities of zeolites A and Y rather than in the α cages or supercages.

In this work, a single crystal of fully Ag^+-exchanged zeolite A (Ag_{12}-A) was treated with KI in CH_3OH solution in an attempt to synthesize a high density of AgI nanoclusters within the zeolite. The structure of the product crystal was determined to verify that nanoclusters had formed, to learn their positions and geometry (including size), and to observe their interactions with the zeolite framework.

Experimental Section

Large colorless single crystals of zeolite 4A (LTA), $Na_{12}Si_{12}Al_{12}O_{48}\cdot 27H_2O$ (Na_{12}-A·$27H_2O$ or Na-A·$27H_2O$) per unit cell were synthesized by Kokotailo and Charnell.[20] Crystals of hydrated Ag_{12}-A (Ag-A) were prepared by the dynamic (flow) ion-exchange of Na-A with aqueous 0.05 M $AgNO_3$ (Aldrich 99.998%) at 294 K.[21,22]

The resulting Ag-A crystal was thoroughly washed with CH_3OH (Merck 99.8%) and then placed in a flowing stream of 0.05 M KI (Aldrich 99.9%) in CH_3OH (Merck 99.8%) at 294 K for 2 days. The crystal was then isolated in its capillary by sealing both ends with a small torch. No attempt was made to dry the CH_3OH beforehand; it has been established that the movement of cations in to and out of a zeolite (ion exchange) is dependent upon the water content of a nonaqueous solvent.[23,24] At the end, no attempt was made to remove the solvent from the crystal, not by evacuation nor by heating. The crystal after ion-exchange with Ag^+ was pale reddish brown. After reaction with KI, it became pale yellow.

Its structure was determined by single-crystal X-ray diffraction techniques at 294(1) K. The cubic space group $Pm\bar{3}m$ (no systematic absences) was used in this work for reasons discussed previously.[25,26] No superstructure reflections ($a = 24.580$ Å, FCC), to support the possible long-range ordering of the Ag_4I_4 nanoclusters (vide infra), were seen; these would have been expected to have substantial intensity. Background intensity was counted at each end of a scan range for a time equal to half the scan time. The intensities of three reflections in diverse regions of reciprocal space were recorded every 3 h to monitor crystal and instrument stability. Only small random fluctuations of these check reflections were observed during the course of data collection. Absorption corrections ($\mu = 5.13$ mm^{-1})[27] were judged to be negligible for this crystal because semiempirical ψ-scans showed only negligible fluctuations for several reflections. A summary of the experimental and crystallographic data is presented in Table 1.

TABLE 1: Summary of Experimental and Crystallographic Data

crystal cross section (mm)	0.08
ion exchange with Ag^+ (days, mL)	2, 10.0
reaction of Ag-A with KI (days, mL)	2, 10.0
no. of reflections for *a*	25
range of reflections for *a*	$20° < 2\theta < 40°$
temperature (K)	294(1)
scan technique	$\theta-2\theta$
scan rate (deg2θ/min)	0.5
scan width (deg2θ)	$0.80 + 0.35 \tan\theta$
$2\theta_{max}$ (deg)	70
unit cell parameter, *a* (Å)	12.290(1)
no. of unique reflections, *m*	877
no. of reflections with $F_o > 4\sigma(F_o)$	264
no. of variables, *s*	50
data/parameter ratio, *m/s*	17.5
weighting parameters: a/b	0.1508/0.0000
final error indices	
R_1[a]	0.077
R_2[b]	0.342
goodness-of-fit[c]	1.11

[a] $R_1 = \sum||F_o| - |F_c||/\sum F_o$ is calculated using only the 264 reflections for which $F_o > 4\sigma(F_o)$. [b] $R_2 = [\sum w(F_o^2 - F_c^2)^2/\sum w(F_o^2)^2]^{1/2}$ is calculated using all 877 unique reflections measured. [c] Goodness-of-fit $= (\sum w(F_o^2 - |F_c|^2)^2/(m - s))^{1/2}$.

Structure Determination. Full-matrix least-squares refinement was done on the structure factors squared (F^2) using all data. Refinement using SHELXL97[28] was initiated with the atomic parameters of the framework atoms [(Si,Al), O(1), O(2), and O(3)] in dehydrated K_{12}-A.[29] The initial refinement using isotropic thermal parameters for all positions converged to the error indices (defined in footnotes to Table 1) $R_1 = 0.33$ and $R_2 = 0.77$. Refinement including the Ag(1) position at a peak (0.1303, 0.1303, 0.1303) opposite a six-ring in the sodalite unit from the initial difference Fourier function led to convergence with $R_1 = 0.26$ and $R_2 = 0.68$ with an occupancy of 1.8(3) Ag^+ ions per unit cell. The next difference Fourier function (based on this model) revealed a peak at (0.2609, 0.2609, 0.2609), opposite a six-ring in the large cavity. Refinement including this peak as K(1) with the occupancy at Ag(1) fixed at 2.0 converged to $R_1 = 0.21$ and $R_2 = 0.58$, with 9.1(5) K^+ ions per unit cell. The addition of another peak at I(1) (0.1210, 0.1210, 0.1210) inside the sodalite unit reduced the error indices to $R_1 = 0.17$ and $R_2 = 0.56$, with occupancies of 2.0 (fixed), 5.9(3), and 1.9(3) for Ag(1), K(1), and I(1), respectively. A subsequent refinement including K(2), a peak found near an eight-ring at (0.0612, 0.4376, 0.5), led to $R_1 = 0.171$ and $R_2 = 0.493$, with occupancies of 2.0 (fixed), 2.0 (fixed), 6.8(4), and 2.5(6) for isotropically refined Ag(1), 1(1), K(1), and K(2), respectively. Inclusion of another peak at I(2), opposite a four-ring at (0.2607, 0.2607, 0.5) in the large cavity, led to $R_1 = 0.148$ and $R_2 = 0.518$, with occupancies of 2.0 (fixed), 2.0 (fixed), 7.8(4), 3.3(6), and 1.5(2) for isotropically refined Ag-(1), I(1), K(1), K(2), and I(2), respectively. A subsequent difference Fourier function based on this model revealed a peak in the large cavity at (0.2170, 0.3174, 0.5) opposite a four-ring. Refinement including this peak as K(3) with fixed occupancies of 2.0, 2.0, and 8.0 at Ag(1), I(1), and K(1) converged to $R_1 = 0.143$ and $R_2 = 0.518$, with occupancies of 3.3(6), 0.9(3), and 2.2(9) at K(2), I(2), and K(3), respectively. When this model was refined with anisotropic thermal parameters for all of the framework atoms [(Si,Al), O(1), O(2), and O(3)] and with fixed occupancies of 2.0, 2.0, 8.0, 3.0, and 1.0 at Ag(1), I(1), K(1),

TABLE 2: Positional, Thermal, and Occupancy Parameters[a]

atom	Wyckoff position	x	*y*	*z*	U_{11}	U_{22}	U_{33}	U_{12}	U_{13}	U_{23}	occupancy[b] fixed	occupancy[b] varied
(Si,AI)	24(*k*)	0	1833(2)	3699(2)	160(15)	125(13)	72(13)	15(11)	0	0	24[c]	
O(1)	12(*h*)	0	2200(11)	5000[d]	577(98)	303(71)	130(60)	0	0	0	12	
O(2)	12(*i*)	0	2967(7)	2967(7)	411(83)	150(41)	150(41)	126(45)	0	0	12	
O(3)	24(*m*)	1127(5)	1127(5)	3395(7)	231(30)	231(30)	434(60)	86(31)	86(31)	59(34)	24	
K(1)	8(*g*)	2577(7)	2577(7)	2577(7)	603(33)	603(33)	603(33)	239(41)	239(41)	239(41)	6	5.9(5)
K(1′)	8(*g*)	2139(15)	2139(15)	2139(15)	271(47)	271(47)	271(47)	183(70)	183(70)	183(70)	2	2.3(5)
Ag(1)	8(*g*)	1423(7)	1423(7)	1423(7)	628(35)	628(35)	628(35)	462(45)	462(45)	462(45)	2	1.8(3)
I(1)	8(*g*)	862(25)	862(25)	862(25)	6123(484)	6123(484)	6123(484)	−1104(305)	−1104(305)	−1104(305)	2	1.9(3)
I(2)	12(*j*)	2662(30)	2662(30)	5000[d]	1617(120)	1399(246)	1399(246)	90(332)	0	0	1	0.9(3)
K(2)	12(*l*)	692(45)	4328(27)	5000[d]	1719(396)	230(156)	1970(453)	0	0	−119(194)	3	3.3(6)
K(3)	24(*l*)	2143(48)	3274(64)	5000[d]	973(453)	1209(552)	452(280)	−11(351)	0	0	2	2.0(6)

[a] Positional parameters X 10^4 and thermal parameters X 10^4 are given. Numbers in parentheses are the estimated standard deviations in the units of the least significant figure given for the corresponding parameter. The anisotropic temperature factor is $\exp[-2\pi^2 a^{-2}(U_{11}h^2 + U_{22}k^2 + U_{33}l^2 + 2U_{12}hk + 2U_{13}hl + 2U_{23}kl)]$. [b] Occupancy factors are given as the number of atoms or ions per unit cell. [c] Occupancy for (Si) = 12, occupancy for (Al) = 12. [d] Exactly 0.5 by symmetry.

K(2), and I(2), respectively, it converged to $R_1 = 0.140$ and $R_2 = 0.506$, with an occupancy of 2.0(6) at K(3). A subsequent refinement with anisotropic thermal parameters for all nonframework positions (Ag(1), I(1), K(1), K(2), I(2), and K(3)) converged to $R_1 = 0.087$ and $R_2 = 0.371$.

Considering the observed content of each sodalite cavity, two Ag^+ and two I^- ions on 3-fold axes opposite four of its eight 6-rings, there must be at least three different kinds of 6-rings per unit cell: two with Ag^+ ions at Ag(1), two with I^- anions at I(1), and four with neither. There should therefore also be (at least) three kinds of K^+ ions at the other side of these six-rings, in the large cavity. In agreement with this, the eight K^+ ions at K(1) were refining with unusually elongated thermal parameters, and another peak was seen near K(1) on the same 3-fold axis in a subsequent difference Fourier function. A refinement with this peak included as K(1′) with occupancies varying at K(1) and K(1′) converged to $R_1 = 0.077$ and $R_2 = 0.347$ with occupancies of 5.9(5) and 2.3(5) at K(1) and K(1′), respectively. A subsequent difference Fourier function did not show any reasonable peaks around K(1) and K(1′), nor around the O(3) framework oxygen position. Attempts to further resolve the K(1) position were unsuccessful.

The final cycles of refinement with occupancies fixed as shown in Table 2 converged to $R_1 = 0.077$ and $R_2 = 0.342$ with anisotropic thermal parameters for all framework and nonframework atoms. Extensive efforts to locate solvent molecules (CH_3OH and likely H_2O) were unsuccessful. Their absence from the structural model is one reason the final *R* values have remained relatively high. The presence of two nonequivalent sodalite cavities, one with Ag_4I_4 and the other without, which could not be crystallographically resolved, is likely to contribute to these high final error indices also. Still, the final difference Fourier function was featureless. All shifts in the final cycles of refinement were less than 0.1% of the corresponding estimated standard deviations. The final structural parameters are given in Table 2, and selected interatomic distances and angles are in Table 3.

Fixed weights were used initially; the final weights were assigned using the formula $w = 1/[\sigma^2(F_o^2) + (aP)^2 + bP]$ where $P = [\max(F_o^2,0) + 2F_c^2]/3$, with $a = 0.151$ and $b = 0.00$ as refined parameters (see Table 1). Atomic scattering factors for Ag, I, K^+, O^-, and $(Si,Al)^{1.75+}$ were used.[30,31] The function describing $(Si,Al)^{1.75+}$ is the mean of the Si^{4+}, Si^0, Al^{3+}, and Al^0 functions. All scattering factors were modified to account for anomalous dispersion.[32,33]

TABLE 3: Selected Interatomic Distances (Å) and Angles (deg)[a]

distances		angles	
(Si,Al)−O(1)	1.661(5)	O(1)−(Si,Al)−O(2)	107.1(6)
(Si,Al)−O(2)	1.659(4)	O(1)−(Si,Al)−O(3)	110.8(4)
(Si,Al)−O(3)	1.676(3)	O(2)−(Si,Al)−O(3)	108.3(3)
		O(3)−(Si,Al)−O(3)	111.4(7)
K(1)−O(3)	2.713(12)		
K(1′)−O(3)	2.341(12)	(Si,A1)−O(1)−(Si,Al)	148.5(9)
Ag(1)−O(3)	2.478(11)	(Si,A1)−O(2)−(Si,Al)	155.7(8)
K(2)−O(1)	2.75(4)	(Si,Al)−O(3)−(Si,Al)	143.7(6)
K(2)−O(2)	3.13(3)		
K(3)−O(1)	2.95(6)	O(3)−K(1)−O(3)	93.2(5)
K(3)−O(3)	3.52(6)	O(3)−K(1′)−O(3)	114.7(6)
		O(3)−Ag(1)−O(3)	105.4(4)
Ag(1)−I(1)	2.973(21)	O(3)−Ag(1)−I(1)	93.1(7),148.9(10)
K(1′)−I(1)	2.72(6)		
K(2)−I(2)	3.17(5)	Ag(1)−I(1)−Ag(1)	112.6(8)
K(1)−I(2)	2.982(10)	I(1)−Ag(1)−I(1)	60.5(16)
I(2)−O(1)	3.32(5)	K(1)−I(2)−K(2)	89.76(14)
I(2)−O(3)	3.32(7)	K(1)−I(2)−K(1)	174.3(21)
		K(2)−I(2)−K(2)	170.5(25)
Ag(1)−K(1)	2.457(21)	K(1′)−I(1)−Ag(1)	144.4(10)

[a] The numbers in parentheses are the estimated standard deviations in the units of the least significant digit given for the corresponding parameter.

TABLE 4: (Si,Al)−O−(Si,Al) Angles (deg)[a] at Framework Oxygens for K^+-Exchanged Zeolite A

K^+-exchanged zeolite A	O(1)	O(2)	O(3)
Dehydrated K_{12}-A[b]	128.5(6)	178.4(5)	153.7(5)
Hydrated K_{12}-A[b]	145.2(9)	159.3(6)	146.0(9)
K_9-A·$(Ag_4I_4)_{0.5}$·K_4I^{3+}	148.5(9)	155.7(8)	143.7(6)

[a] The numbers in parentheses are the estimated standard deviations in the units of the least significant digit given for the corresponding parameter. [b] Data from ref 29.

Results and Discussion

Zeolite A Framework. The flex of (distortions to) the framework in this structure is much more like that of hydrated K_{12}-A than that of dehydrated K_{12}-A (see Table 4).[29] This indicates that this structure contains a substantial amount of occluded material (e.g., AgI, KI, and perhaps solvent molecules) like the H_2O molecules in hydrated K_{12}-A.[29]

K^+ Ions. A K^+ ion in the large cavity lies on a 3-fold axis opposite each of the eight 6-rings per unit cell. However, from the viewpoint of the sodalite cavity, there should be three different kinds of 6-rings (four empty, two near Ag(1), and two near I(1)), and therefore three different K^+ positions on the 3-fold axes in the large cavity. Unfortunately, only the K(1)

TABLE 5: Deviations of Ions (Å) from the (111) Plane at O(3)[a]

	K_9-A·$(Ag_4I_4)_{0.5}$·K_4I^{3+}	dehydrated K_{12}-A[b]
K(1)	1.48	0.79
K(1′)[c]	0.55	
Ag(1)	−0.98	
I(1)[c]	−2.17	

[a] A positive deviation indicates that the ion lies in the large cavity. A negative deviation indicates that the ion lies on the same side of the plane as the origin, i.e., inside the sodalite unit. [b] Data from ref 29. [c] K(1′) and I(1) form 0.55 + 2.17 = 2.72 Å bonds along 3-fold axes through 6-rings.

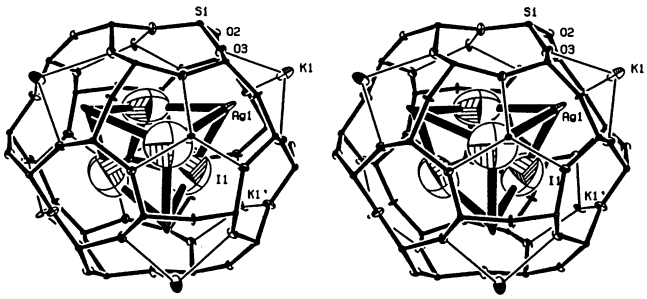

Figure 1. Stereoview of a sodalite unit in K_9-A·$(Ag_4I_4)_{0.5}$·K_4I^{3+}. Half of the sodalite cavities contain a Ag_4I_4 cluster as shown. Each Ag^+ cation coordinates octahedrally to three I(1) iodine ions and three O(3) framework oxygens. Each iodide ion coordinates tetrahedrally to three Ag^+ ions and to one K^+ ion at K(1′). The zeolite-A framework is drawn with medium bonds between oxygens and tetrahedrally coordinated (Si,Al) atoms. Ellipsoids of 20% probability are shown.

and K(1′) positions have been resolved. With occupancies of 6 and 2, respectively, the K^+ positions opposite the (otherwise) empty 6-rings and either those opposite the Ag^+ ions or those opposite the I^- ions have not been resolved.

K(1) is 2.713(12) Å from its three O(3) oxygens, but K(1′) is much closer, 2.341(12) Å, to its O(3) oxygens (see Table 3). Considering the sum of the ionic radii of K^+ and O^{2-}, 1.33 + 1.32 = 2.65 Å,[34,35] respectively, the K(1)−O(3) approach distances are somewhat long but reasonable. The K(1′)-O(3) distances, however, are much shorter than this sum. It follows that the K(1) and K(1′) ions extend very different distances, 1.48 and 0.55 A, respectively, into the large cavity from the (111) planes at O(3) (see Table 5), and make very different angles with O(3), O(3)−K(1)−O(3) = 93.2(5)° and O(3)−K(1′)−O(3) = 114.7(6)°.

Why are the two K^+ ions at K(1′) so close to the O(3) oxygens? Because of intercationic repulsion, it cannot be to approach the two Ag^+ ions at Ag(1). It also cannot be to approach (two of the four) empty 6-rings unusually closely. It must therefore be to approach the two I^- ions at I(1). Supporting this is the unusually short 2.72-Å K(1′)-I(1) approach distance (see Figure 1). This through-the-6-ring bond is even shorter than the sum of the K^+ and I^- ionic radii, 1.33 + (1.65 to 2.20) = 2.98 to 3.53 Å, respectively. It follows that it is the four K^+ ions opposite 6-rings that are empty on their sodalite-unit sides, and those that contain Ag^+ ions there, that are unresolved at the K(1) position.

Three K^+ ions at K(2) occupy the three 8-rings per unit cell. Each lies 0.85 Å from its 8-ring plane. Each K(2) ion is 2.75(4) Å from one O(1) oxygen and 3.13(3) Å from two O(2) oxygens of an 8-ring (see Figure 2). Similar unequal coordination of 8-ring oxygens to K^+ ions, but with a lesser degree of inequality, was seen in the crystal structures of hydrated and dehydrated K_{12}-A.[29]

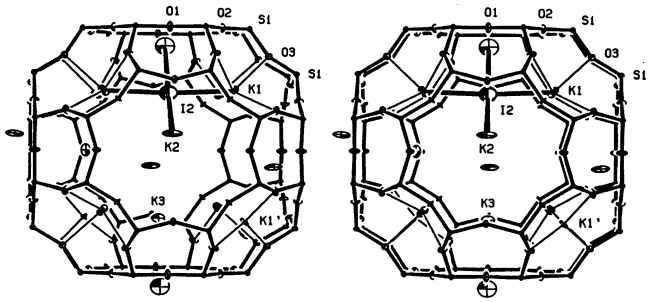

Figure 2. Stereoview of the large cavity of K_9-A·$(Ag_4I_4)_{0.5}$·K_4I^{3+} with an iodide ion bonded to four K^+ ions. See the caption to Figure 1 for other details.

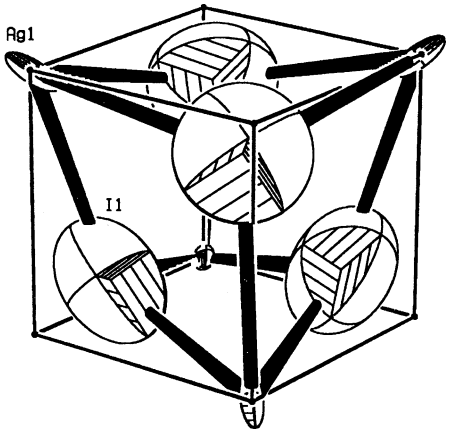

Figure 3. The Ag_4I_4 cluster (symmetry T_d) found in half of the sodalite cavities. Its distortion (puckered cube or interpenetrating tetrahedra) can be seen from the original cube drawn with fine lines. See the caption to Figure 1 for other details.

The K(3) position is new: it was found neither in hydrated nor dehydrated K_{12}-A. It is occupied by two K^+ ions per unit cell opposite 4-rings in the large cavity (see Figure 2). Each is 2.95(6) Å from two O(1) oxygens.

Ag_4I_4 Nanocluster in the Sodalite Unit. The Ag^+ ions at Ag(1) are each 2.478(11) Å from three 6-ring oxygens at O(3) (see Table 3). This distance is approximately the sum of the ionic radii of Ag^+ and O^{2-}, 1.13 + 1.32 = 2.45 Å,[34,35] respectively. These Ag^+ ions are recessed 0.98 Å into the sodalite unit from the (111) planes at O(3) (see Table 5). In contrast, the I^- ions at I(1) are recessed much further, 2.17 Å, into the sodalite unit from these planes (see Table 5). Thus the iodide ions are far from the three nearest anionic framework oxygens, as would be expected for anions.

A Ag^+ ion and an I^- ion cannot approach the same 6-ring because their interionic distance, 1.20 Å, would be impossibly short. The possible contact distances between I^- ions within the same sodalite unit are 2.12(6), 3.00(9), and 3.67(8) Å. Considering the I^- radius (1.65 to 2.20 Å[34,35]), only the two latter contact distances are possible. Therefore, I^- ions cannot occupy adjacent 6-rings in the sodalite cavity.

Considering the possible arrangements of I^- and Ag^+ ions within the sodalite unit, an interpenetrating tetrahedral (puckered cubic) arrangement of four Ag^+ and four I^- ions in half of the sodalite units is most likely (see Figures 1 and 3). It gives the greatest number of bonds per ion (12 bonds per 8 ions), the most regular coordination geometries (only mildly distorted octahedral for Ag^+ and tetrahedral for I^-), and is consistent with the symmetry of the Ag(1) and I(1) positions (both lie on 3-fold axes). In this arrangement, each Ag^+ ion bonds to three

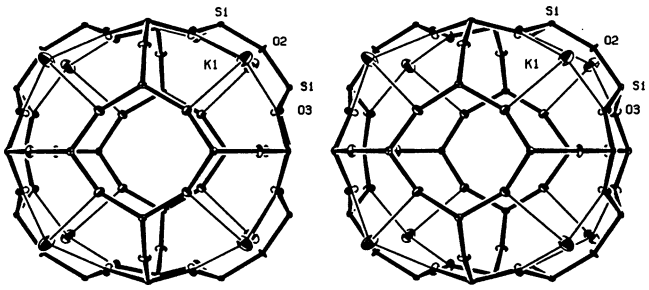

Figure 4. Stereoview of an empty sodalite cavity with 8 K^+ cations at K(1). See the caption to Figure 1 for other details.

I^- ions (in addition to three framework oxygens), and each I ion bonds to three Ag^+ ions (in addition to one K(I′) ion). The Ag(1)−I(1) distance, 2.973(21) Å, lies within the range expected for the sum of the Ag^+ and I^- radii, 2.78 to 3.33 Å (r_{Ag^+} = 1.13 Å; r_{I^-} ranges from 1.65 to 2.20 Å).[34,35] In Cs_2AgI_3,[35] the Ag−I distance is 2.78 Å, indicating that the I^- radius is 2.78−1.13 = 1.65 Å in that compound.

The resulting neutral Ag_4I_4 nanocluster has T_d symmetry and would be well stabilized by the interactions of each its four Ag^+ ions with three 6-ring oxygens (Ag(1)−O(3) = 2.478(11) Å). In addition, as can be seen in Figure 1, each I^- ion coordinates to a K(1′) cation through a 6-ring. Ag_4I_4 is ca. 8.0 Å in diameter.

Silver iodide can be obtained under ambient conditions in both the zinc blende and the wurzite structures, both of which have Ag−I distances of 2.74 Å.[36,37] The Ag_4I_4 group has been found at the core of a series of compounds, $(Ph_3P)_4Ag_4X_4$ (X = Cl, Br, and I).[38] It was described as a 'cubane-like' structure defined by two interpenetrating silver and X tetrahedra situated on alternate corners of a highly distorted cube (as is seen here (see Figures 1 or 3)), with each silver atom being further coordinated to a triphenylphosphine ligand.[38] In the crystal structure of $(Ph_3P)_4Ag_4I_4$,[38] the average Ag−I distance is 2.911 Å (range 2.837(2) to 3.038(3) Å). This is longer than the 2.74-Å distance seen in both forms of AgI,[36,37] but close to 2.973(21) Å, the value found in this structure.

Half of the sodalite cavities in the crystal are empty (see Figure 4). Each is surrounded by eight K^+ ions at K(1). Perhaps it follows that the Ag_4I_4 clusters are ordered as the stoichiometry indicates, at least in the short range, filling alternate sodalite cavities (see Figure 5). This material (the zeolite framework, the cations, and the clusters) appears to be stoichiometric, suggesting that this or a similarly prepared material would have very well defined physical properties. The single crystal studied, a cube about 80 μm on an edge, contained more than 100 Tera (10^{14}) Ag_4I_4 clusters.

Another crystal with a higher Ag_4X_4 content, with Ag_4Br_4, was prepared; unfortunately its crystallinity had deteriorated in preparation.

K_4I^{3+} Cluster in the Large Cavity. One iodide ion per unit cell is found at I(2), on a 2-fold axis opposite a 4-ring in the large cavity. It bonds to four K^+ ions, two at K(1) and two at K(2), in a near square-planar manner to give a K_4I^{3+} cluster (see Figures 2 and 6).

K(1)−I(2) = 2.982(10) and K(2)−I(2) = 3.17(5) Å; the bond angles about I(2) are given in Table 2. For comparison, the sum of the ionic radii of K^+ and I^- is, respectively, 1.33 + (1.65 to 2.20) = 2.98 to 3.53 Å.[34,35] The iodide ion at I(2) is recessed ca. 0.20 Å from the $K(1)_2K(2)_2$ plane toward the center of the large cavity, probably because of repulsive interactions with the O(1) and O(3) framework oxygens which are only 3.32(5) and 3.32(7) Å away, respectively (see Table 3 and Figure 2).

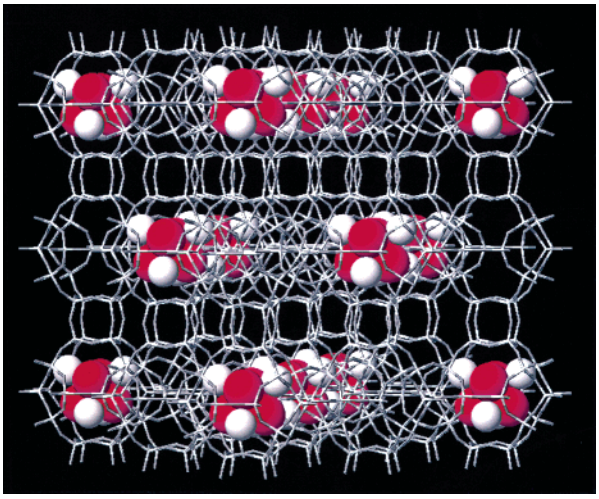

Figure 5. The Ag_4I_4 clusters in alternating sodalite cavities of several unit cells. For clarity, the framework atoms have been simplified and the K^+ and K_4I^{3+} cations have been omitted. The long-range ordering and identical orientations of the nanoparticles shown here is reasonable, but it has not been established in this work.

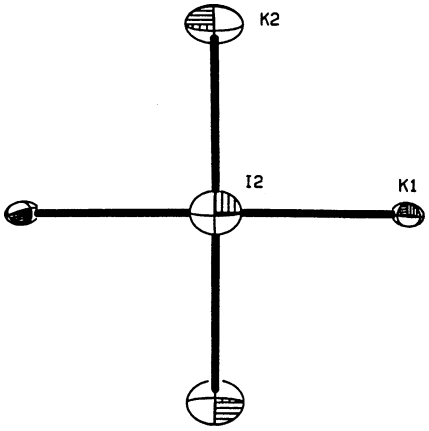

Figure 6. K_4I^{3+}. An iodide ion bonded to four K^+ ions in a near square planar manner in the large cavity. See the caption to Figure 1 for other details.

To coordinate to I(2), the 8-ring K^+ ions at K(2) have moved closer to the iodide ion and out of the planes of their 8-rings. In this way, three K^+ ions have cooperated to capture one KI molecule per unit cell.

Because of the presence of the I(2) anion, there should be three (rather than two) nonequivalent K^+ ions unresolved at K(1), and two at K(2).

Net Reactions. The net reactions that occurred during sample preparation are therefore

$$(\text{in } H_2O)\ Na_{12}\text{-A} + 12Ag^+ \rightarrow Ag_{12}\text{-A} + 12Na^+ \quad (1)$$

and

$$(\text{in wet } CH_3OH)\ Ag_{12}\text{-A} + 13K^+ + 3I^- \rightarrow K_9\text{-A}\cdot(Ag_4I_4)_{0.5}\cdot K_4I^{3+} + 10Ag^+ \quad (2)$$

Summary

Ag_4I_4 nanoclusters with T_d symmetry have been synthesized in half of the sodalite cavities of K−A by the reaction of Ag-A and KI in CH_3OH. One KI molecule per unit cell is retained deep in each large cavity as part of a nearly square planar K_4I^{3+} ion.

Acknowledgment. We gratefully acknowledge the support of the Central Laboratory of Kyungpook National University for its diffractometer and computing facilities. This work was supported by a Korea Research Foundation Grant (KRF-2000-137-D00139).

Supporting Information Available: Observed and calculated structure factors for K_9-A·$(Ag_4I_4)_{0.5}$·K_4I^{3+}. This material is available free of charge via the Internet at http://pubs.acs.org.

References and Notes

(1) Bhatia, S. *Zeolite Catalysis: Principles and Applications*, CRC Press: Boca Raton, Florida, 1988; pp 1−2.
(2) Smith, J. V. "Origin and structure of zeolites" in *Zeolite Chemistry and Catalysis*; Rabo, J. A., Ed.; *Am. Chem. Soc. Monogr.*, 1976; 171, Chapter 1, pp 3−4.
(3) Srdanov, V. I.; Blake, N. P.; Markgraber, D.; Metiu, H.; Stucky, G. D. *Advanced Zeolite Science and Applications, Studies in Surface Science and Catalysis*; Jansen, J. C., Stocker, M., Karge, H. G., Weitkamp, J., Eds.; Elsevier Science: Amsterdam, 1994; Vol. 85, pp 115−144.
(4) Terasaki, L.; Yamazaki, K.; Thomas, J. M.; Ohsuna, T.; Watanabe, D.; Sanders, J. V.; Barry, J. C. *Nature (London)* **1987**, *330*, 58−60.
(5) Stucky, G. D.; MacDougall, J. E. *Science* **1990**, *247*, 669−678.
(6) Alekseev, Yu. A.; Bogomolov, V. N.; Zhukova, T. B.; Petranovskii, V. P.; Romanov, S. G.; Kholodkevich, S. V. *Izv. Akad. Nauk. SSSR, Ser Fiz.* **1986**, *50*, 418−423.
(7) Wang, Y.; Herron, N. *J. Phys. Chem.* **1987**, *91*, 257−260.
(8) Wang, Y.; Herron, N. *J. Phys. Chem.* **1988**, *92*, 4988−4994.
(9) Herron, N.; Wang, Y.; Eddy, M. M.; Stucky, G. D.; Cox, D. E.; Moller, K.; Bein, T. *J. Am. Chem. Soc.* **1989**, *111*, 530−540.
(10) Stein, A.; Ozin, G. A.; Stucky, G. D. *J. Am. Chem. Soc.* **1992**, *114*, 8119−8129.
(11) Stein, A.; Ozin, G. A.; Stucky, G. D. *J. Am. Chem. Soc.* **1990**, *112*, 2, 904−905.
(12) Kodaira, T.; Ikeda, T.; Takeo, H. *Eur. Phys. J. D* **1999**, *9*, 601−604.
(13) Chen, W.; Wang, Z.; Lin, Z.; Lin, L.; Fang, K.; Xu, Y.; Su, M.; Lin, J. *J. Appl. Phys.* **1998**, *83*, 3811−3815 and references therein.
(14) Tani, T.; Murofushi, M. *J. Imag. Sci. Technol.* **1994**, *38*, 1−9.
(15) Takahashi, K.; Miyahara, J.; Shibahara, Y. *J. Electrochem. Soc.* **1985**, *132*(6), 1492−1494.
(16) Hirono, T.; Yamada, T. Japanese Patent 61-061894, 1986.
(17) Godber, J.; Ozin, G. A. *J. Phys. Chem.* **1988**, *92*, 4980−4987.
(18) Hirono, T.; Kawana, A.; Yamada, T. *J. Appl. Phys.* **1987**, *62*, 1984−1988.
(19) Zhai, Q. Z.; Qiu, S.; Xiao, F. S.; Zhang, Z. T.; Shao, C. L.; Han, Y. *Mater. Res. Bull.* **2000**, *35*, 59−73.
(20) Charnell, J. F. *J. Cryst. Growth* **1971**, *8*, 291−294.
(21) Kim, Y.; Seff, K. *J. Phys. Chem.* **1978**, *82*, 1071−1077.
(22) Kim, Y.; Seff, K. *J. Am. Chem. Soc.* **1978**, *100*, 6989−6997.
(23) Bae, D.; Seff, K. *Zeolites* **1996**, *17*, 444−446.
(24) Ho, K.; Lee, H. S.; Leano, B. C.; Sun, T.; Seff, K. *Zeolites* **1995**, *15*, 377−381.
(25) Cruz, W. V.; Leung, P. C. W.; Seff, K. *J. Am. Chem. Soc.* **1978**, *100*, 6997−7003.
(26) Mellum, M. D.; Seff, K. *J. Phys. Chem.* **1984**, *88*, 3560−3563.
(27) *International Tables for X-ray Crystallography;* Ibers, J. A., Hamilton, W. C., Eds.; Kynoch Press: Birmingham: England, 1974; Vol. IV, pp 61−66.
(28) Sheldrick, G. M., *SHELXL97, Program for the Refinement of Crystal Structures*, University of Gottingen, Germany, 1997.
(29) Leung, P. C. W.; Kunz, K. B.; Seff, K.; Maxwell, I. E. *J. Phys. Chem.* **1975**, *79*, 2157−2162.
(30) Doyle, P. A.; Turner, P. S. *Acta Crystallogr., Sect. A* **1968**, *24*, 390−397.
(31) *International Tables for X-ray Crystallography;* Ibers, J. A., Hamilton, W. C., Eds.; Kynoch Press: Birmingham, England, 1974; Vol. IV, 71−98.
(32) Cromer, D. T. *Acta Crystallogr.* **1965**, *18*, 17−23.
(33) *International Tables for X-ray Crystallography*; Ibers, J. A., Hamilton, W. C., Eds.; Kynoch Press: Birmingham: England, 1974; Vol. IV, pp 148−150.
(34) Emsley, J. *The Elements*; Oxford University Press: Oxford, 1990; 176−177.
(35) *Tables of Interatomic Distances and Configuration in Molecules and Ions*; The Chemical Society: London, 1958.
(36) Wells, A. F. *Structural Inorganic Chemistry*, 5th ed.; Clarendon Press: Oxford, 1986; p 410.
(37) Chateau, H. *Compt. Rend.* **1959**, *249*, 1638.
(38) Teo, B.-K.; Calabrese, J. C. *J. Am. Chem. Soc.* **1975**, *97*, 1256−1257.